Journal of General Virology (2005), **86**, 2553–2561 DOI 10.1099/vir.0.81021-0

Early endocytosis pathways in SSN-1 cells infected by dragon grouper nervous necrosis virus

Wangta Liu,[1] Chi-Hsin Hsu,[1] Yi-Ren Hong,[2] Shu-Chuan Wu,[2] Chun-Hsiung Wang,[1] Yi-Min Wu,[1] Chia-Ben Chao[3] and Chan-Shing Lin[1]

[1]Department of Marine Biotechnology and Resources, National Sun Yat-sen University, Kaohsiung 804, Taiwan

[2]Graduate Institute of Biochemistry, Kaohsiung Medical University, Kaohsiung, Taiwan

[3]Institute for Animal Disease Prevention and Control, Kaohsiung, Taiwan

Correspondence
Chan-Shing Lin
shinlin@mail.nsysu.edu.tw

Received 10 March 2005
Accepted 16 May 2005

Many fish undergo betanodavirus infection. To study the infection process of dragon grouper nervous necrosis virus (DGNNV), native virus and virus-like particles (VLPs) were used to analyse the binding and internalization in SSN-1 cells. The binding of DGNNV and VLPs to SSN-1 cells was demonstrated using Western blotting and immunofluorescence microscopy. As estimated by indirect ELISA, the DGNNV particles bound SSN-1 cells in a dose-dependent manner up to 8×10^4 particles per cell. The binding of VLPs was sensitive to neuraminidase and tunicamycin, suggesting that cell-surface sialic acid is involved in binding. The penetration of DGNNV into cells, which was monitored by electron microscopy, appeared to occur mainly via the spherical pit and membrane ruffling pathways. Occasionally, a spherical pit was engulfed by membrane ruffling so as to form a large figure-of-eight-shaped vesicle with an open connection. Our observations suggest that DGNNV utilizes both micro- and macropinocytosis pathways to enter SSN-1 cells.

INTRODUCTION

Piscine nodaviruses are classified in the genus *Betanodavirus* and have been associated with disease in many species of marine fish in Asia, Europe and Australia (Munday & Nakai, 1997; Munday *et al.*, 2002). Diseased fish are typically diagnosed as having viral encephalopathy and retinopathy or viral nervous necrosis, and clinical symptoms include abnormal swimming behaviour, darkening of the skin, and mass mortality in both larvae and juveniles raised in hatcheries.

The Malabar grouper (*Epinephelus malabaricus*) nervous necrosis virus (MGNNV) is a member of the genus *Betanodavirus* and the virions consist of 180 molecules of a single-capsid protein that encapsulates a bipartite genome comprised of single-stranded positive RNAs, RNA1 (~3·1 kb) and RNA2 (~1·4 kb) (Mori *et al.*, 1992; Lin *et al.*, 2001). It is presumed that RNA1 encodes the viral replicase, whilst RNA2 has been shown to encode the capsid protein (Lin *et al.*, 2001). The capsid protein sequences of dragon grouper nervous necrosis virus (DGNNV) and MGNNV are 99 % identical. Non-enveloped T = 3 quasi-symmetric virus-like particles (VLPs) have been generated by baculovirus expression of the MGNNV capsid protein (Lin *et al.*, 2001; Tang *et al.*, 2002). The DGNNV capsid protein expressed in *Escherichia coli* also forms VLPs that morphologically resemble native virions (Lu & Lin, 2003). The VLPs can block the attachment of native virions to the surface of SSN-1 cells, thus restricting virus infection (Lu *et al.*, 2003), suggesting that the outer shell of VLPs is structurally indistinguishable from native virions.

Animal viruses employ a variety of cell-specific invasion mechanisms for propagation: attachment, endocytosis, endosomal escape, cytoplasmic transport, disassembly and import into nuclei (Smith & Helenius, 2004). Attachment to the cell surface is the initial step in the infection process, followed by either direct penetration through the plasma membrane or endocytosis. There are many examples of specific virus–cell interactions determining tissue tropism. Initial binding and invasion, for example, involve virus recognition of specific attachment factors, receptors and co-receptors (Müller *et al.*, 1995). Endocytosis, in which virus particles traverse the plasma membranes of susceptible cells, usually occurs via four major routes: clathrin-coated vesicles, the caveolar pathway, macropinocytosis, and novel non-clathrin- and non-caveolae-dependent endocytosis (Kirchhausen, 2000; McPherson *et al.*, 2001; Sieczkarski & Whittaker, 2002). In the early phase, endocytosis generally initiates the formation of spherical vesicles that subsequently fuse into other cytosolic compartments such as the early and late endosomes. Enveloped viruses can penetrate the cell by fusion with the lipid envelope of the cell membrane (Dimitrov, 2000), whereas non-enveloped viruses escape from endocytic vesicles by

either disrupting the membrane (Nemerow, 2000) or inducing the formation of pores (Belnap *et al.*, 2000), through which the viral genome and requisite accessory factors can be delivered to the cytosol.

Piscine nodaviruses are considered to have a restricted tissue and host tropism (Comps *et al.*, 1996; Iwamoto *et al.*, 2004). Antibody-mediated neutralization of virus infectivity supports the hypothesis that the cell–virus binding involves specific interactions (Lai *et al.*, 2001; Mori *et al.*, 2003). Furthermore, we have previously demonstrated that VLPs block DGNNV binding to SSN-1 cells (Lu *et al.*, 2003). In comparison with the model for poliovirus, it has been hypothesized for the entry pathway of the insect nodaviruses that only the genomic ssRNA is delivered into the cytosol via a pore formed at the point of contact of a viral shell and the cell membrane, based upon the evidence of a single puff structure in the virus particle (Johnson & Rueckert, 1997). In contrast to the insect nodavirus model, however, the endocytosis pathway utilized by piscine nodaviruses has not been examined. Here, we have studied DGNNV binding to SSN-1 cells and mechanisms of internalization by using electron microscopy.

METHODS

DGNNV and VLP preparation. DGNNV, isolated originally from *Epinephelus lanceolatus*, was propagated in SSN-1 cells (Frerichs *et al.*, 1991) for 4 days, after which the cell cultures were frozen and thawed three times (Lin *et al.*, 2001). Cell debris was removed by centrifugation at 39 500 ***g*** for 20 min (Hitachi CR20B2). The supernatant was layered onto a 30 % (w/w) sucrose cushion and ultracentrifuged at 300 000 ***g*** for 1 h (Hitachi SCP70G) to obtain a virus pellet free of cellular proteins.

To prepare VLPs, the pDA8-transformed *E. coli* JM109 (Lu *et al.*, 2003) were grown at 30 °C in Luria–Bertani broth containing 100 μg ampicillin ml^{-1}. When the cell density reached an OD_{600} of 0·2–0·3, 0·84 mM IPTG was added. After induction for 2 h, the cells were harvested by centrifugation (5150 ***g***, 4 °C, 20 min), resuspended in Dulbecco's (D)-PBS (2·67 mM potassium chloride, 1·47 mM potassium phosphate, 137·93 mM sodium chloride, 8·1 mM sodium phosphate, pH 7·3), and then lysed by three passages through a French press (Avestin Emulsiflex-C5). Cell debris in the lysate was removed immediately by centrifugation at 39 500 ***g*** for 20 min (Hitachi CR20B2). The supernatant was then layered onto a 30 % (w/w) sucrose cushion and ultracentrifuged at 300 000 ***g*** for 1 h (Hitachi SCP70G). The VLP pellet was resuspended in D-PBS and further purified by ultracentrifugation in a 20–38 % (w/w) CsCl gradient (Hitachi SCP70G) at 100 000 ***g*** for 12 h. The particles present in the gradient fractions were visualized by electron microscopy.

VLP-binding assay by Western blotting and ELISA. SSN-1 cells grown to confluence as monolayers were suspended in D-PBS containing 0·5 mM EDTA. The concentration of SSN-1 cells was adjusted with D-PBS to 3×10^6 cells ml^{-1}. All subsequent steps were conducted on ice or at 4 °C. A total of 50 μl quantified VLPs was added to 100 μl cell suspension and incubated for 1 h on a rotating wheel. Following centrifugation at 4000 r.p.m. for 5 min (Hettich Universal 32R), unbound particles in the supernatant were quantified using an indirect ELISA, while cell-bound VLPs were detected by Western blotting. For detection of the VLP protein, cell pellets were washed with D-PBS and lysed in 40 μl sample buffer for 10 min in boiling water. Aliquots (20 μl) of cell-VLP protein lysate were analysed by SDS-PAGE. After transfer onto a nitrocellulose membrane, the capsid protein was detected with rabbit anti-VLP antiserum (Lu & Lin, 2003) and goat anti-rabbit peroxidase-conjugated IgG. A chemiluminescent signal, stained using ECL Western blotting detection reagent (Amersham), was detected using a luminescent image analyser (Fujifilm LAS-3000). For the ELISA, 96-well microtitre plates were coated with supernatant containing unbound particles at 4 °C overnight. The plates were washed and blocked with 2 % BSA in D-PBS, followed by incubation with a rabbit anti-VLP antiserum (1 : 1000) and goat anti-rabbit peroxidase-conjugated IgG (1 : 3000; Amersham). After colour development by the addition of 100 μl 3,3′,5,5′ tetramethylbenzidine substrate (Pierce), the A_{450} values were measured in an automated ELISA reader (Bio-Rad model 550). The particle number was estimated using the formula: numbers of cell-bound particles = Avogadro's number × bound particles (g)/molecular mass of a VLP (g $mole^{-1}$).

Treatment with *N*-glycosylation inhibitor. SSN-1 cells were cultured in 24-well plates (3×10^5 cells per well) in L15 medium supplemented with 10 % fetal bovine serum (FBS) and tunicamycin (2 μg ml^{-1}) for 24 h. Following removal of the medium and washing, the cell monolayers were incubated with purified virus or VLPs for 1 h. The cells were then washed to remove unbound virus/VLPs and resuspended in 20 μl D-PBS. Proteins present in cell lysates were analysed by SDS-PAGE in a 12 % gel. The proteins were transferred to a nitrocellulose membrane, and detected with rabbit anti-VLP antiserum, goat anti-rabbit peroxidase-conjugated IgG and ECL chemiluminescent detection reagents as described earlier. The density of the stained protein at 37 kDa was estimated with a Multi Gauge programme (Fujifilm).

Neuraminidase and trypsin treatment of SSN-1 cells. SSN-1 cells grown to monolayers were suspended in D-PBS containing 0·5 mM EDTA. After one wash, the cells were diluted to a concentration of 3×10^6 ml^{-1} in D-PBS. An aliquot (100 μl) of the cell suspension was treated at 27 °C for 30 min with either 900 mU neuraminidase (Sigma) ml^{-1} or 0·05 % trypsin/0·5 mM EDTA (Gibco). All subsequent steps were performed on ice or at 4 °C. The cells were centrifuged, washed with D-PBS, resuspended in 100 μl virus or VLP solution (1 μg), and incubated for 1 h on a rotating wheel. After centrifugation to remove unbound particles, cells were collected (4000 r.p.m., 5 min; Hettich Universal 32R) and subjected to SDS-PAGE in a 12 % gel. VLP protein was detected by Western blotting and chemiluminescence, as described earlier.

Indirect immunofluorescence assay. SSN-1 cells were seeded onto coverslips (3×10^5 cells per slide) and grown for 20 h in L15 with 10 % FBS. The medium was removed and the cells were incubated with either 100 μg VLPs or virus in D-PBS containing 0·1 % BSA for 1 h at 27 °C. The cells were fixed with ice-cold methanol after several washes with D-PBS to remove unbound VLPs or virus. The slides were then incubated with rabbit anti-VLP antiserum for 1 h, given several washes with D-PBS and incubated with 1 : 500 goat anti-rabbit IgG-dithioaminofluorescein conjugate (Rockland) for 1 h. Unbound secondary antibody was removed by washing with D-PBS. The cells were covered with a drop of mounting medium (Sigma) and sealed with nail polish. Photographs were taken using a fluorescent microscope (Olympus BX 40).

Immunoelectron microsopy. To visualize the uptake of virions or VLPs, 6×10^5 SSN-1 cells were seeded in a 24-well plate and then incubated for 20 h at 27 °C. The plate was chilled on ice, and the medium was replaced by D-PBS containing 0·05 % BSA to which 10 μg ml^{-1} of virus or VLPs had been added. After incubation for 1 h, unbound particles were removed by four washes with ice-cold D-PBS. The cells were incubated with rabbit anti-VLP antiserum for 40 min, washed with PBS, and incubated with goat anti-rabbit

IgG-gold conjugate (18 nm; Jackson) for another 40 min. The cells were shifted to 27 °C for various intervals. The reaction was stopped by fixation of the cells with 4 % paraformaldehyde, 2·5 % glutaraldehyde. After washing with D-PBS, the cells were treated with 1 % osmium tetroxide in D-PBS. The cells were dehydrated in solutions containing gradually increasing concentrations of ethanol, and then embedded in epoxide resin. The resins, in which the cells were embedded on the bottom edge, were removed from the wells; subsequently, the samples were turned at a 90° angle for a second embedding, so that the cells were relocated to the centre of the specimen. Ultrathin sections (90 nm) were prepared using an Ultracut (Reichert), stained with 1 % uranyl acetate and lead acetate, and examined using a JEOL electron microscope (JEM-2000 EX II).

RESULTS

VLP binding by SSN-1 cells

It has been demonstrated experimentally that DGNNV VLP can block cell attachment and infection by native virus (Lu *et al.*, 2003). To quantify VLPs attaching to SSN-1 cells under cold-binding conditions, an ELISA was used to detect the amount of unbound VLPs in the supernatant and thus estimate the number of VLPs bound to each SSN-1 cell. ELISA detection of coat protein showed that the quantity of bound VLPs per cell increased linearly as VLP number increased, indicating a proportional dose-dependent binding of VLPs to the cells (Fig. 1a). As one VLP is composed of 180 monomers of 37 kDa capsid protein, dose-dependent binding occurred below an estimated 8×10^4 VLPs per cell. The association of VLPs to cells was also examined by Western blot detection of the 37 kDa capsid protein, which also indicated that the amount of cell-associated capsid protein increased proportionally with the amount of VLP added to the cells (Fig. 1b).

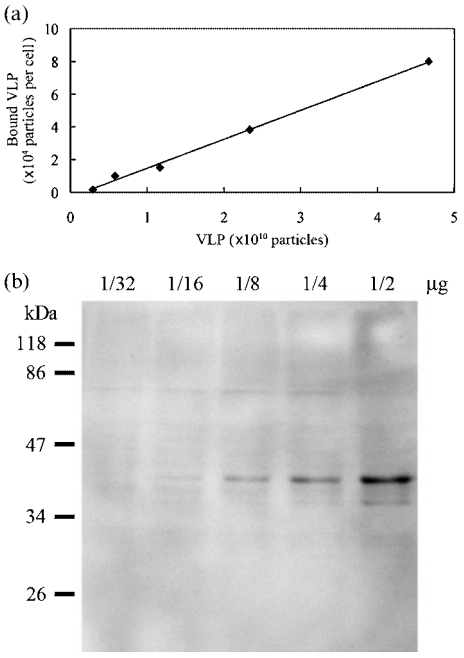

Fig. 1. Binding of VLPs to SSN-1 cells. (a) Increasing amounts of VLPs were incubated with 3×10^5 SSN-1 cells for 1 h. Unbound particles remaining in the supernatant were quantified using an ELISA. (b) The 37 kDa capsid protein of VLPs attached to cells was detected, following 12 % SDS-PAGE, transferred to a nitrocellulose membrane and subjected to Western blotting with chemiluminescent detection as described in Methods.

Sialic acid of *N*-glycosylated receptor is involved in DGNNV binding

To examine the nature of the cellular surface component(s) involved in virus binding, the SSN-1 cells were grown in the presence of tunicamycin to block *N*-glycosylation of cellular proteins. As shown in Fig. 2(a), Western blot detection of the 37 kDa capsid protein indicated that binding of virus and VLPs decreased approximately 70 % after the cells had been treated with 2 μg tunicamycin ml^{-1} at 27 °C for 24 h.

To identify whether the glycosylated surface receptor might contain sialic acid for protection from protease digestion, SSN-1 cells were treated with either neuraminidase or trypsin. The reactions to remove the sialic acid by neuraminidase were carried out at 27 °C for 30 min. The VLPs bound to the enzyme-treated cells were analysed by Western blotting. As shown in Fig. 2(b), the amounts of VLP or virus capsid protein associated with SSN-1 cells significantly decreased approximately 80 % after treatment of the cells

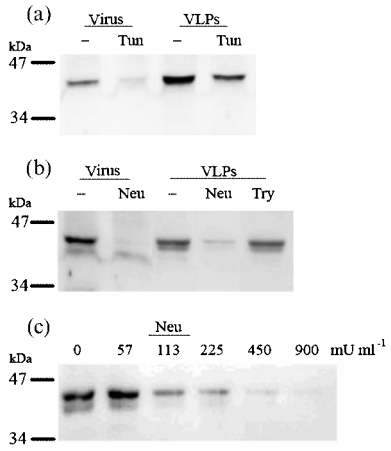

Fig. 2. *N*-glycosylation of the receptor(s) participating in DGNNV virion and VLP binding. (a) SSN-1 cells were cultured in L15 medium supplemented with tunicamycin (Tun) and 10 % FBS for 24 h. The cells were incubated with virus or VLPs for 1 h and the 37 kDa capsid protein was detected using Western blotting. (b) Cells were cultured in L15 medium, 10 % FBS for 20 h and treated with either 900 mU neuraminidase (Neu) ml^{-1} or 0·05 % trypsin (Try). (c) Cells were cultured in L15 medium, 10 % FBS for 20 h and treated with various concentrations of neuraminidase for 30 min. After treatments cells were incubated with virus or VLPs for 1 h in a rotator at 4 °C. After washing away unbound particles, cellular bound-VLPs and virus were detected using Western blotting.

with 900 mU neuraminidase ml^{-1}. However, after treatment of the cells with 0·05 % trypsin at 27 °C for 30 min, no reduction in VLP-binding occurred (Fig. 2b). To further evaluate neuraminidase-mediated reduction in VLP binding, SSN-1 cells were treated with different concentrations of neuraminidase ranging from 57 to 900 mU ml^{-1}. Western blotting revealed that the amount of VLP capsid protein present in the treated cells decreased significantly as the concentrations of neuraminidase increased (Fig. 2c).

Presence of virions or VLPs in SSN-1 cells observed by immunofluorescence assay

The binding of native DGNNV virions and VLPs to SSN-1 cells was examined by fluorescence microscopy using anti-VLP antiserum as the primary antibody. Fluorescence covering the whole cell surface was detected after incubation with either native virus or VLPs, but not in their absence. In addition, densely fluorescent spots were observed in some cells incubated with either DGNNV virions or VLPs (Fig. 3). The fluorescent spots of virus-binding cells tended to cluster together to one side of the cells (shaped like caps), while the spots of VLP-binding cells were rather scattered over whole cells with spots of small granular appearance.

Ultrastructure analysis of DGNNV virion endocytosis in SSN-1 cells

To examine the early phase of DGNNV attachment and entry into SSN-1 cells, electron microscopy was employed. After incubating cell monolayers with virus particles on ice for 1 h, examination of the representative sections showed that the plasma membrane was covered with virus particles (Fig. 4a and b). The physical images also depict high viral multiplicity binding in one cell as the quantitative data shown in Fig. 1(a).

In sections from cells that were warmed at 27 °C for 15 min to promote virus entry into cells, several regular invaginations and a few unique rufflings were identified in the plasma membrane (Fig. 4c). The membrane invagination formed spherical pits, up to 200 nm in diameter. Virus-containing vesicles in the cytoplasm resembled endosomes. However, they were irregular and bigger in diameter (0·5–1·4 μm) compared with normal endosomes (Fig. 4c). As shown in Fig. 4(d), ruffled membrane regions were associated with clustered virus particles (Fig. 4d, left panel), while some clusters of virus particles endocytosed in the cytosol were contained inside irregularly sized, membrane-associated compartments (Fig. 4d, middle and right panels).

After incubation at 27 °C for 45 min, only a few virus particles were identified at plasma membranes, while most particles occurred within endocytic vesicles located inside the cytosol (Fig. 5a). Fig. 5(b) hinted at a possible clue for the virus entry process and showed vesicle membrane that appeared to be degenerating from intact, to partially broken, and finally vanishing while releasing viral genome (Fig. 5b; left, middle and right panels, respectively).

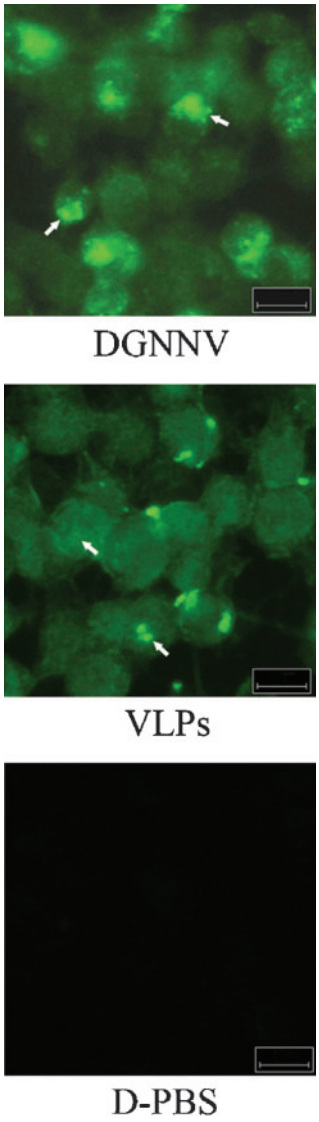

Fig. 3. Immunofluorescence detection of DGNNV and VLPs bound to SSN-1 cells. Cells grown on coverslips were incubated with DGNNV or VLPs for 1 h at 27 °C (D-PBS as control). After several washes with D-PBS to remove unbound particles, cells were fixed with ice-cold methanol. The binding of cells immunoreactive for anti-VLP antiserum was visualized using fluorescent microscopy. Arrows highlight the presence of cap-like spots (DGNNV) and patches (VLPs). Bars, 10 μm.

Internalization of VLPs

As virus replication is generally rapid, electron microscopy images obtained with virus-treated cells warmed for 45 min (Fig. 5) do not conclusively demonstrate that the clusters of virus particles in vesicles were due to internalization rather than replication. To confirm that warming had

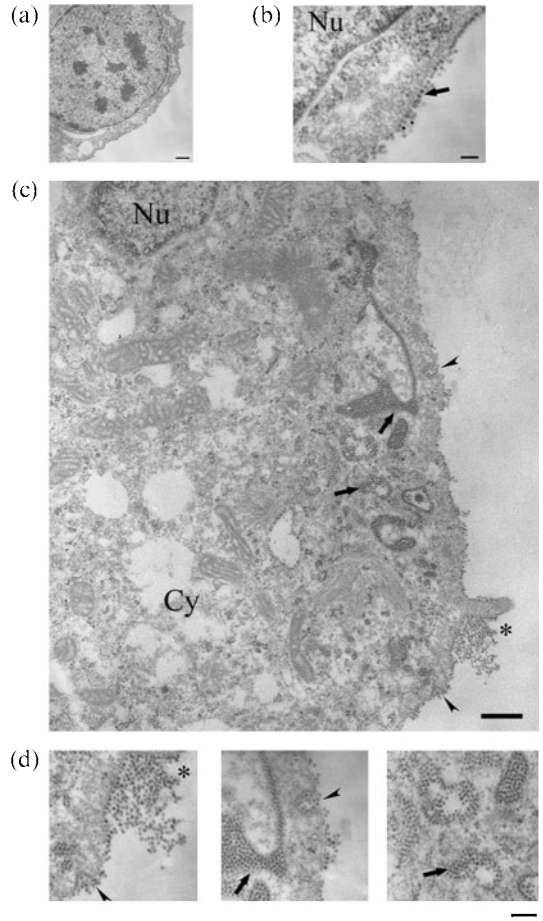

Fig. 4. Electron microscopy of DGNNV entry into SSN-1 cells. As shown in panels (a) and (b), the samples were incubated with the virus at 0 °C for 1 h, without a temperature shift. As shown in panels (c) and (d), the samples were incubated at 0 °C for 1 h and then shifted to 27 °C for 15 min to initiate virus internalization. Unbound particles were washed away using D-PBS and the cells fixed with 4 % paraformaldehyde, 2·5 % glutaraldehyde. Ultrathin sections were prepared for electron microscopy as described in Methods. Nu, nucleus; Cy, cytoplasm. Arrows highlight the presence of virus particles, while arrowheads depict the presence of pits (c and d). Asterisk (*) in panels (c) and (d) indicates a ruffled membrane associated with clustered virus particles. Bars, 500 nm (a); 100 nm (b); 500 nm (c) and 200 nm (d).

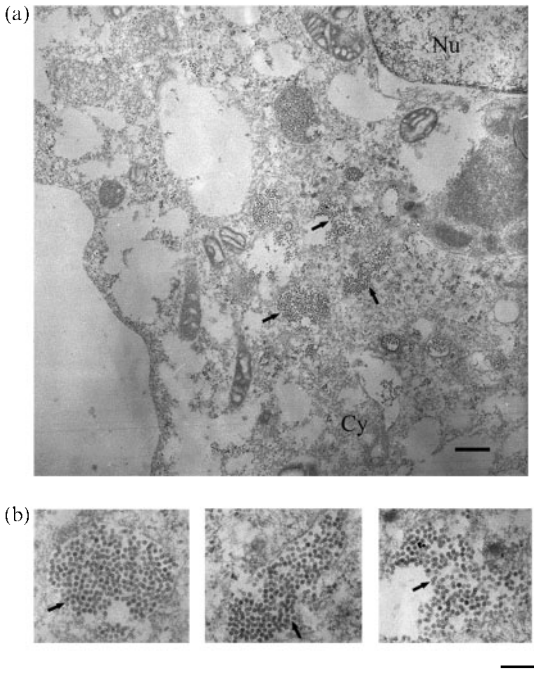

Fig. 5. Aggregations of DGNNV particles in SSN-1 cells. Cells were incubated with DGNNV for 1 h on ice, and then shifted to 27 °C for 45 min. The cells were fixed with 4 % paraformaldehyde, 2·5 % glutaraldehyde and prepared for electron microscopy as described in Methods. Nu, nucleus; Cy, cytoplasm. Arrows highlight the presence of virus particles. Bars, 500 nm (a) and 200 nm (b).

induced virion internalization, non-replicating VLPs were substituted for virus particles and the experiments were repeated. Electron microscopy of VLP-treated SSN-1 cells following warming clearly showed disproportionate endosomes containing clusters of VLPs, which were often aligned along their outer membrane (Fig. 6). In Fig. 6(a), a rod-shaped vesicle containing densely packed VLPs shows evidence of fusion with a membrane of a large empty vesicle (indicated by an arrow), and their emergence in the cytosol (arrowhead). Endosomes in which some of the membrane appears to have disappeared but in which particles were still clustered were also observed (Fig. 6b, arrow). The observation revealed that the DGNNV indeed internalize whole particle into cytosol.

DISCUSSION

DGNNV appears to enter SSN-1 cells via spherical pits and membrane ruffling. Electron microscopy identified spherical invagination with no evidence of an electron-dense coat and the ruffling morphology appears to be consistent with macropinocytosis (Maniak, 2003). Typically, the diameter of a macropinosome is 0·5–5 μm, while in the early phase micropinocytic vesicles are less than 200 nm in diameter. Macropinocytosis refers to the formation of large, irregular primary endocytic vesicles by the closure of lamellipodia, primarily generated at ruffled membrane domains. Although there is no direct evidence with respect to the dynamic structures and composition of disproportionate macropinosomes, we incubated SSN-1 cells with non-replicating VLPs for different warming periods to observe virion internalization. In our observations, upon cellular attachment and the entry of DGNNV virions and VLPs, a single pseudopod, or lamellipodium, forms and appears to bend back toward the cell surface, thereby possibly trapping a large area containing membrane-associated particles. Ruffles might be further characterized by their

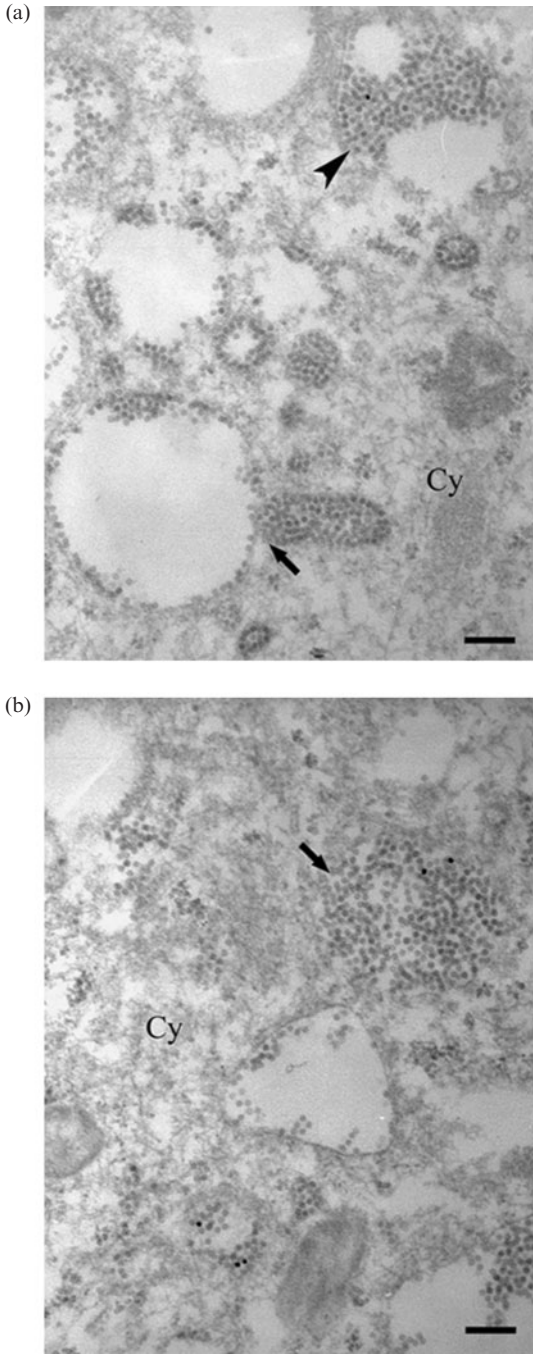

Fig. 6. VLP internalization in SSN-1 cells visualized by electron microscopy. Cells were incubated with VLPs for 1 h on ice, and then shifted to 27 °C for 45 min. The cells were fixed and prepared for electron microscopy as described in Methods. Cy, cytoplasm. Arrows point to the presence of VLP-containing vesicles and the arrowhead shows their emergence into the cytosol. Bars, 200 nm.

different compositions that were enriched in the ruffling membrane, such as phosphoinositides and raft lipid markers (Mañes *et al.*, 1999; Hurley & Meyer, 2001). On the other hand, several spherical pits of DGNNV virion endocytosis were identified to be a normal size like other viruses (<200 nm) (Bousarghin *et al.*, 2003). Although we did not explicitly observe the electron-dense coat on the inside face of spherical pits, a possible clathrin-mediated pathway still cannot be excluded. The characteristics of spherical pits should be verified by clathrin-specific antibody, inhibitors of endocytosis, and molecular inhibitor of dominant-negative proteins, as well as gene knock-out experiments (Sieczkarski & Whittaker, 2002).

Several kinds of membrane ruffling and large disproportionate macropinosomes were observed in DGNNV-infected cells (see Figs 4, 5 and 6). From images captured by electron microscopy, we propose that three macropinosome types are the results of variations in the manner they formed. Firstly, a large ruffle following formation of regular spherical pits seems to lead to the development of figure-of-eight-shaped macropinosomes (Fig. 7a). Similarly, it has been mentioned that the clathrin-coated pit of adenovirus-infected cells occurs simultaneously with

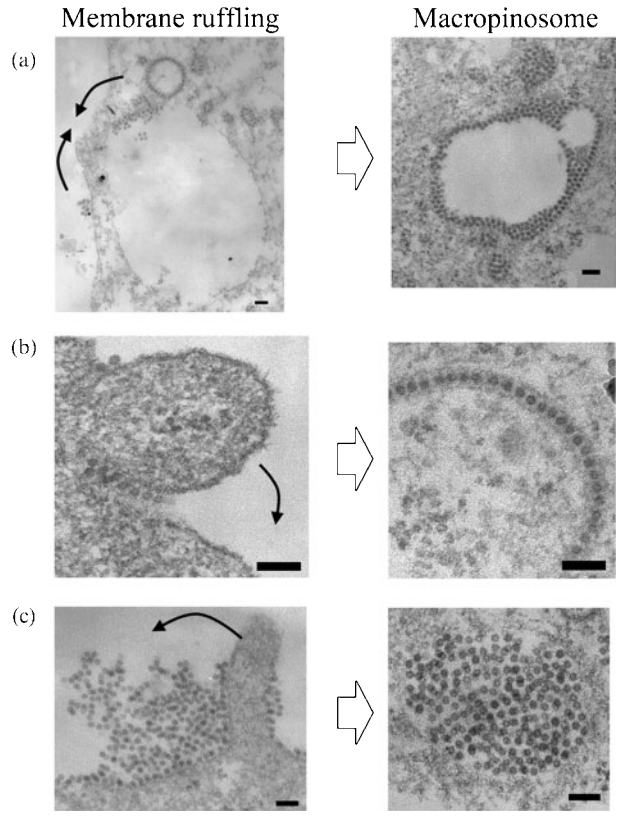

Fig. 7. Proposed dynamics of membrane ruffling related to subsequent macropinocytosis. (a) A large ruffle engulfs a pit to form a figure-of-eight-shaped vesicle. (b) A thick ruffle of membrane squeezes the particle-associated membrane to form a chain-shaped vesicle. (c) A ruffle encloses a cluster of particles to form a circular virus-packed macropinosome. Arrows in the left panel represent possible movements of different ruffles. Bars, 100 nm.

macropinocytosis in its surrounding area (Meier *et al.*, 2002). Secondly, a thick ruffle that squeezes the plasma membrane may form a thread-like membrane gap, which creates chain-shaped macropinosomes (Fig. 7b). Thirdly, a ruffle enclosing clusters of virus particles might form circular virus-packed macropinosomes (Fig. 7c). In the three mechanisms we propose, the small pits may activate ruffling enclosure of the figure-of-eight-shaped macropinosomes; on the other hand, close threaded alignment of virus particles provides a chance for the formation of the chain-shaped macropinosomes, while the particle aggregations help the formation of virus-packed-type circular macropinosomes.

ELISA quantification of VLP-cell binding indicates that DGNNV can attach to the SSN-1 cell surface in very high numbers (8×10^4 VLPs per cell). Other viruses can bind to cells in the same order of magnitude, such as 3000 sites per HeLa cell for poliovirus (Bibb *et al.*, 1994), 16 000 sites for adenovirus (White, 1993), 20 000 VLPs for human papillomavirus (Volpers *et al.*, 1995) and 60 000 sites for rhinovirus (Greve *et al.*, 1989). Furthermore, the electron microscopy of VLP- or DGNNV virion-treated cells showed that the cell plasma membrane was physically covered by the icosahedron particles. Therefore, high multiplicity of DGNNV virion binding on the SSN-1 is consistently supported by the results from ELISA and electron microscopy.

Such cap-like spots in immunofluorescence microscopy (see Fig. 2) have been depicted as a characteristic of the virus binding, a similar phenomenon has been demonstrated to be associated with receptor-mediated endocytosis in human papillomavirus type 33 (Volpers *et al.*, 1995). Virus propagation might gather the virion particles in one location, making cap-like spots stand out. In incubation with non-replicating VLPs, nevertheless, whole cells were still covered by fluorescent spots. To moderate the effects of virus propagation, we decreased the period of warming and employed non-replicating VLPs to observe the early phase of internalization by using electron microscopy. It appears likely that the virus particles jammed inside the vesicles were at the early stage of endocytosis, not a result of virus propagation. Electron microscopy also revealed that DGNNV can enter SSN-1 cells via two routes: inward pit formation and outward membrane ruffling. This is the first report that fish betanodavirus can employ both of these entry mechanisms, in which virus particles are delivered into cells within vesicles and remain intact inside the cytosol. This suggests that the viral genomic RNAs are released into cytosol from virions inside or released from the vesicles, rather than from virus particles located on the outer plasma membrane. We also observed vesicles in which the membrane had disintegrated, releasing intact virus particles into the cytosol, which does not support the hypothesis proposed for insect nodavirus that only the ssRNA genome is delivered into the cytosol (Johnson & Rueckert, 1997). This may not be a surprise possibility because the virion structures and capsid proteins of the two nodavirus families are quite different, as described elsewhere (Tang *et al.*, 2002). With respect to the mechanisms by which fish nodaviruses release their genome into the cytosol, however, additional studies are required to determine how the infectosome releases its genome from vesicles.

We have shown that neuraminidase can remove the ligand of cell surface component(s) to prevent DGNNV virion attachment. This indicates that the sialic acid of the components is essential for DGNNV binding because neuraminidase cleaves *N*-acetylneuraminic acid (sialic acid) from a variety of glycoproteins (Hatton & Regoeczi, 1973). The tunicamycin pretreatment enervated SSN-1 causing the cells to bind virus particles incompetently, implying that glycoprotein is involved in the viral entry because tunicamycin can inhibit the transfer of UDP-GlcNAc to dolichol-1-phosphate, an early step in the synthesis of the ligand precursor for the *N*-glycosylation pathway. One might argue that the frequent inward and outward movement of the pseudopod lamellipodia of SSN-1 cells, similar to macrophage phagocytosis, could accidentally result in a non-specific engulfment of virus particles that pre-attach to the membrane. However, this argument of random engulfment is not supported by the virion binding disability of enzyme-treated cells mentioned above, and is contrary to the finding that VLPs can specifically block DGNNV attachment to SSN-1 cells (Lu *et al.*, 2003). Furthermore, Iwamoto *et al.* (2004) have identified capsid proteins as host-specificity determinants in betanodaviruses by using reassortants of RNA2 between striped jack nervous necrosis virus and sevenband grouper nervous necrosis virus. We hypothesize, therefore, that the attachment of piscine nodavirus to SSN-1 cells is specifically receptor-mediated, according to the findings that tunicamycin and neuraminidase markedly reduce DGNNV binding to SSN-1 cells. It has been demonstrated in the human papillomavirus that a similar phenomenon is characteristic of the binding of multivalent ligands to a specific membrane protein that promotes receptor-mediated endocytosis (Volpers *et al.*, 1995). Even in conventional phagocytosis, microbes that are apposed on the cell membrane are also specifically engulfed by receptor-mediated pseudopods (Rittig *et al.*, 1998). Phagocytosis-like ruffling of DGNNV virion macropinocytosis is not necessarily non-specific. On the other hand, trypsinization of the cells prior to the addition of particles did not decrease the VLP-binding ability of SSN-1 cells, which may suggest that no suitable peptide bond of the virus-binding glycoprotein is exposed for the protease to digest (Volpers *et al.*, 1995). However, a non-protein receptor cannot be excluded until the receptor molecule is fully identified.

There is possibly an alternative mechanism for the formation of macropinosomes, in which the virus attachment autonomously stimulates the movement of plasma membrane. A variety of macropinosomes may be formed, according to the manner in which the virus attachment provokes the movement of cell membrane. In adenovirus infection, it has been shown that the clathrin-coated pit

associates with the virus, triggering macropinocytosis in the surrounding area (Meier & Greber, 2004). It has been suggested by tunicamycin inhibition and neuraminidase treatment that DGNNV virion internalization in the presence of macropinocytosis is a specifically receptor-mediated process. The effects of an overdose infection on the formation of macropinosomes cannot be ruled out, because overdose infection could unnaturally exert irritating stresses on the cell membrane artificially creating an event *in vitro* that does not exist *in vivo*. The macropinocytosis subsequently only occurs in the presence of high-dose infection. Conceptually, a single virion might be sufficient to infect and propagate in a cell, in which membrane ruffling may not be a necessary mechanism for virus uptake. In such a case, biochemical marker molecules of macropinocytosis would be required to support the argument in terms of low dose of infection. Provided that macropinocytosis does not naturally occur in low-dose viral infection, the biomarkers will prove useful to elucidate the native functions of macropinocytosis, and its association with high-dose infection.

ACKNOWLEDGEMENTS

This project was partially supported by grants from the National Science Council, Taiwan (NSC92-2313-B-110-005) and the University Integration Programme from the Ministry of Education (93RA04602). Pacific Edit reviewed the manuscript prior to submission.

REFERENCES

Belnap, D. M., Filman, D. J., Trus, B. L. & 8 other authors (2000). Molecular tectonic model of virus structural transitions: the putative cell entry states of poliovirus. *J Virol* **74**, 1342–1354.

Bibb, J. A., Witherell, G., Bernhardt, G. & Wimmer, E. (1994). Interaction of poliovirus with its cell-surface binding site. *Virology* **201**, 107–115.

Bousarghin, L., Touzé, A., Sizaret, P. Y. & Coursaget, P. (2003). Human papillomavirus types 16, 31, and 58 use different endocytosis pathways to enter cells. *J Virol* **77**, 3846–3850.

Comps, M., Trindade, M. & Delsert, C. (1996). Investigation of fish encephalitis viruses (FEV) expression in marine fishes using DIG-labelled probes. *Aquaculture* **143**, 113–121.

Dimitrov, D. S. (2000). Cell biology of virus entry. *Cell* **101**, 697–702.

Frerichs, G. N., Morgan, D., Hart, D., Skerrow, C., Roberts, R. J. & Onions, D. E. (1991). Spontaneously productive C-type retrovirus infection of fish cell lines. *J Gen Virol* **72**, 2537–2539.

Greve, J. M., Davis, G., Meyer, A. M., Forte, C. P., Yost, S. C., Marlor, C. W., Kamarck, M. E. & McClelland, A. (1989). The major human rhinovirus receptor is ICAM-1. *Cell* **56**, 839–847.

Hatton, M. W. & Regoeczi, E. (1973). A simple method for the purification of commercial neuraminidase preparations free from proteases. *Biochim Biophys Acta* **327**, 114–120.

Hurley, J. H. & Meyer, T. (2001). Subcellular targeting by membrane lipids. *Curr Opin Cell Biol* **13**, 146–152.

Iwamoto, T., Okinaka, Y., Mise, K., Mori, K. I., Arimoto, M., Okuno, T. & Nakai, T. (2004). Identification of host-specificity determinants in betanodaviruses by using reassortants between striped jack nervous necrosis virus and sevenband grouper nervous necrosis virus. *J Virol* **78**, 1256–1262.

Johnson, J. E. & Rueckert, R. R. (1997). Packaging and release of viral genome. In *Structural Biology of Viruses*, pp. 269–287. Edited by W. Chiu, R. M. Burnett & R. L. Garcea. New York: Oxford University Press.

Kirchhausen, T. (2000). Three ways to make a vesicle. *Nat Rev Mol Cell Biol* **1**, 187–198.

Lai, Y. S., Chiu, H. C., Murali, S., Guo, I. C., Chen, S. C., Fang, K. & Chang, C. Y. (2001). *In vitro* neutralization by monoclonal antibodies against yellow grouper nervous necrosis virus (YGNNV) and immunolocalization of virus infection in yellow grouper, *Epinephelus awoara* (Temminck & Schlegel). *J Fish Dis* **24**, 237–244.

Lin, C. S., Lu, M. W., Tang, L., Liu, W., Chao, C. B., Lin, C. J., Krishna, N. K., Johnson, J. E. & Schneemann, A. (2001). Characterization of virus-like particles assembled in a recombinant baculovirus system expressing the capsid protein of a fish nodavirus. *Virology* **290**, 50–58.

Lu, M. W. & Lin, C. S. (2003). Involvement of the terminus of grouper betanodavirus capsid protein in virus-like particle assembly. *Arch Virol* **148**, 345–355.

Lu, M. W., Liu, W. & Lin, C. S. (2003). Infection competition against grouper nervous necrosis virus by virus-like particles produced in *Escherichia coli*. *J Gen Virol* **84**, 1577–1582.

Mañes, S., Mira, E., Gómez-Moutón, C., Lacalle, R. A., Keller, P., Labrador, J. P. & Martínez-A, C. (1999). Membrane raft microdomains mediate front–rear polarity in migrating cells. *EMBO J* **18**, 6211–6220.

Maniak, M. (2003). Macropinocytosis. In *Endocytosis*, pp. 78–93. Edited by M. Marsh. New York: Oxford University Press.

McPherson, P. S., Kay, B. K. & Hussain, N. K. (2001). Signaling on the endocytic pathway. *Traffic* **2**, 375–384.

Meier, O. & Greber, U. F. (2004). Adenovirus endocytosis. *J Gene Med* **6**, S152–S163.

Meier, O., Boucke, K., Hammer, S. V., Keller, S., Stidwill, R. P., Hemmi, S. & Greber, U. F. (2002). Adenovirus triggers macropinocytosis and endosomal leakage together with its clathrin-mediated uptake. *J Cell Biol* **158**, 1119–1131.

Mori, K. I., Nakai, T., Muroga, K., Arimoto, M., Mushiake, K. & Furusawa, I. (1992). Properties of a new virus belonging to nodaviridae found in larval striped jack (*Pseudocaranx dentex*) with nervous necrosis. *Virology* **187**, 368–371.

Mori, K., Mangyoku, T., Iwamoto, T., Arimoto, M., Tanaka, S. & Nakai, T. (2003). Serological relationships among genotypic variants of betanodavirus. *Dis Aquat Organ* **57**, 19–26.

Müller, M., Gissmann, L., Cristiano, R. J., Sun, X. Y., Frazer, I. H., Jenson, A. B., Alonso, A., Zentgraf, H. & Zhou, J. (1995). Papillomavirus capsid binding and uptake by cells from different tissues and species. *J Virol* **69**, 948–954.

Munday, B. L. & Nakai, T. (1997). Special topic review: nodaviruses as pathogens in larval and juvenile marine finfish. *World J Microbiol Biotechnol* **13**, 375–381.

Munday, B. L., Kwang, J. & Moody, N. (2002). Betanodavirus infections of teleost fish: a review. *J Fish Dis* **25**, 127–142.

Nemerow, G. R. (2000). Cell receptors involved in adenovirus entry. *Virology* **274**, 1–4.

Rittig, M. G., Jagoda, J. C., Wilske, B., Murgia, R., Cinco, M., Repp, R., Burmester, G. R. & Krause, A. (1998). Coiling phagocytosis discriminates between different spirochetes and is enhanced by phorbol myristate acetate and granulocyte-macrophage colony-stimulating factor. *Infect Immun* **66**, 627–635.

Sieczkarski, S. B. & Whittaker, G. R. (2002). Dissecting virus entry via endocytosis. *J Gen Virol* **83**, 1535–1545.

Smith, A. E. & Helenius, A. (2004). How viruses enter animal cells. *Science* **304**, 237–242.

Tang, L., Lin, C. S., Krishna, N. K., Yeager, M., Schneemann, A. & Johnson, J. E. (2002). Virus-like particles of a fish nodavirus display a capsid subunit domain organization different from that of insect nodaviruses. *J Virol* **76**, 6370–6375.

Volpers, C., Unckell, F., Schirmacher, P., Streeck, R. E. & Sapp, M. (1995). Binding and internalization of human papillomavirus type 33 virus-like particles by eukaryotic cells. *J Virol* **69**, 3258–3264.

White, J. M. (1993). Integrins as virus receptors. *Curr Biol* **3**, 596–599.